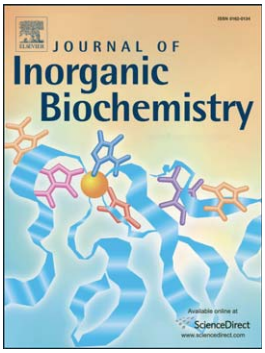

Unbound Position II in MXCXXC Metallochaperone Model Peptides Impacts Metal Binding Mode and Reactivity: Distinct Similarities to Whole Proteins

Michal S. Shoshan, Noa Dekel, Wojciech Goch, Deborah E. Shalev, Tsafi Danieli, Mario Lebendiker, Wojciech Bal, Edit Y. Tshuva

PII: S0162-0134(16)30041-1
DOI: doi: 10.1016/j.jinorgbio.2016.02.016
Reference: JIB 9930

To appear in: *Journal of Inorganic Biochemistry*

Received date: 12 October 2015
Revised date: 19 January 2016
Accepted date: 10 February 2016

Please cite this article as: Michal S. Shoshan, Noa Dekel, Wojciech Goch, Deborah E. Shalev, Tsafi Danieli, Mario Lebendiker, Wojciech Bal, Edit Y. Tshuva, Unbound Position II in MXCXXC Metallochaperone Model Peptides Impacts Metal Binding Mode and Reactivity: Distinct Similarities to Whole Proteins, *Journal of Inorganic Biochemistry* (2016), doi: 10.1016/j.jinorgbio.2016.02.016

Unbound Position II in MXCXXC Metallochaperone Model Peptides Impacts Metal Binding Mode and Reactivity: Distinct Similarities to Whole Proteins

Michal S. Shoshan[a], Noa Dekel[b], Wojciech Goch[c], Deborah E. Shalev[b], Tsafi Danieli[b], Mario Lebendiker[b], Wojciech Bal[c] and Edit Y. Tshuva[a*]

[a]Institute of Chemistry, The Hebrew University of Jerusalem, Edmond J. Safra Campus, Jerusalem 9190401, Israel

[b]Wolfson Centre for Applied Structural Biology, The Hebrew University of Jerusalem, Edmond J. Safra Campus, Jerusalem 9190401, Israel

[c]Institute of Biochemistry and Biophysics, Polish Academy of Sciences, Warszawa 02106, Poland

Abstract: The effect of position II in the binding sequence of copper metallochaperones, which varies between Thr and His, was investigated through structural analysis and affinity and oxidation kinetic studies of model peptides. A first Cys-Cu(I)-Cys model obtained for the His peptide at acidic and neutral pH, correlated with higher affinity and more rapid oxidation of its complex; in contrast, the Thr peptide with the Cys-Cu(I)-Met coordination under neutral conditions demonstrated weaker and pH dependent binding. Studies with human antioxidant protein 1 (Atox1) and three of its mutants where S residues were replaced with Ala suggested that (a) the binding affinity is influenced more by the binding sequence than by the protein fold (b) pH may play a role in binding reactivity, and (c) mutating the Met impacted the affinity and oxidation rate more drastically than did mutating one of the Cys, supporting its important role in protein function. Position II thus plays a dominant role in metal binding and transport.

Keywords: Cu • peptides • metalloproteins • NMR • Atox1

*Corresponding author:
Edit Y. Tshuva
edit.tshuva@mail.huji.ac.il
Fax: +972-2-6584282

1. Introduction

Copper ions are found in all living organisms in two valence states: Cu(I) and Cu(II), and are involved in a variety of beneficial functions due to the metal redox reactivity. Nevertheless, the rapid change between copper oxidation states may also produce toxic reactive oxygen species (ROS) according to the Haber-Weiss reaction (Eq. 1).[1-8] Therefore, copper ions in the biological environment are protected by binding proteins.

(1) $Cu^{+} + H_2O_2 \rightleftharpoons Cu^{2+} + OH^{-} + OH^{\cdot}$

Copper metallochaperone cellular proteins, such as the human cytoplasmic protein Atox1 or its yeast analogue Atx1, preclude harmful reactions by binding Cu(I) and inhibiting oxidation to Cu(II).[8-19] These proteins contain the conserved binding sequence *MH/TCX$_1$X$_2$C* (single letter amino acid code, X represents any amino acid). Based on all structures analyzed thus far, including dimers analyzed by X-ray[16] and monomers analyzed by NMR with Cys–Cu(I) binding constraints,[20-26] these proteins were reported to bind the metal ion via two thiolato groups of the soft cysteine residues;[13-15, 17-18] Additionally, positively charged Lys at position ~60 apparently neutralizes the resulting negative ligated metal center.[13] Interestingly, despite the highly conserved nature of the Met residue in all proteins known from this family, and the high affinity of Cu(I) to S ligands, Met participation in metal binding was never observed for Cu metallochaperones; only its effects on protein hydrophobicity and flexibility have been proposed,[9, 11, 20, 22, 27-29] although Met contribution to Cu(I) affinity was noticed.[27, 30]

Modeling chemistry is a widely used method to simplify the investigation of a biological process.[13] Peptides with the conserved binding sequence of copper metallochaperones were previously investigated,[31-34] as models for the natural system.[13, 35-36] A peptide that included the Atx1 binding sequence with Thr at position II was analyzed by NMR without prior assumptions on metal binding mode, and showed that actually, the Met residue bound the Cu(I) metal under acidic and neutral pH, along with only one thiolato group of the proximate Cys in a pseudo linear coordination mode (M1 and C3; Figure 1a). However, under basic conditions the coordination changed to presumably give the Cys,Cys coordination (C3 and C6; Figure 1b).[31] A pH-dependent binding and release mechanism was hypothesized to affect the ion transportation.[31, 37] Nevertheless, when position II in the model peptide was Asp as in the analogous Zn(II) metallochaperone

ZntA,[32, 38] the Asp residue bound the copper under both acidic and basic conditions[32] even though the carboxylato group is a hard ligand that should not bind tightly soft metals such as Cu(I); thus, position II influenced the binding mode of the peptide by participating in the coordination.

The human metallochaperone Atox1 delivers the Cu(I) metal ion to the trans-Golgi copper transporters ATP7A and ATP7B by an unknown mechanism,[16, 41] dysfunction of which induces Menkes and Wilson's diseases, respectively.[16, 42-47] Affinity studies of these proteins to Cu(I) showed that the ion transport to its target protein is driven by gradient of affinities.[19] These transporters contain six metal binding domains (MBDs) where all, except the third domain, have Thr at position II as in yeast Atx1 and human Atox1, while the third domain has His at this position. The reason for this difference is yet unknown, but the third domain has a dissociation constant that is higher by two orders of magnitude than those of the other MBDs.[19]

It is thus of interest to evaluate the effect of residue His at position II of the binding sequence on metal coordination. Although the N donors of His are relatively hard ligands for the soft Cu(I) metal, its binding could not be ruled out, especially considering the Asp binding observed previously for the analogous model,[32] and the binding of His to Cu(I) in a related protein, CopZ, that includes His in its binding sequence.[48] Therefore, herein we investigated the structure and properties of a model peptide with His at position II, and analyzed it together with its Thr analogue with otherwise identical sequence. The NMR structure of the His model along with affinity and oxidation kinetic studies point to strong influence of position II on peptide reactivity, while demonstrating the first fully determined Cys-Cu(I)-Cys model peptide obtained under neutral conditions. Additionally, analysis of the wild type whole-protein Atox1 and three of its mutants provided additional insights on the protein function.

2. Materials and Methods

2.1. General

Unless otherwise stated, all chemicals were purchased from Sigma-Aldrich. The peptides were purchased from Biochimica Ltd. (Montreal, Quebec, Canada) or from JPT Peptide Technologies GmbH (Berlin, Germany) with a purity of >95% by HPLC.

2.2. Sample Preparation for Structural Determination by NMR

The head-to-tail cyclic peptide with the sequence MHCSGCSRPG (5.0 mg, 5.0 μmol) was dissolved in triple distilled water (TDW; 810 μL) and D_2O (100 μL) and the pH was adjusted by using a stock solution of NaOH (0.1 M) and determined by pH indicator sticks as 3.0, 6.7, 7.3 or 8.3. The solution was divided into two equimolar solutions; the first was further diluted to a total volume of 500 μL with TDW (final peptide concentration: 5 mM) and used as the apo-sample; the second was treated with a stock solution of CuCl in TDW (45 μL, 56 mM) (final peptide and CuCl concentrations: 5 mM each) representing the bound peptide sample.

Accurate-Mass Q-TOF LC/MS measurements were carried on an Agilent Technologies 6520 (mass accuracy <2.0 ppm) through direct injections. The samples were prepared under conditions identical to those used for NMR measurements. The conditions included a temperature of 350 K and a fragmentor voltage of 150 V. Theoretical m/z values: 1016.21 for peptide only ($C_{38}H_{61}N_{15}O_{12}S_3$), 1079.75 for peptide with copper ion ($C_{38}H_{59}N_{15}O_{12}S_3Cu$).[49]

2.3. NMR structural determination

NMR experiments were performed on a Bruker Avance 600 MHz DMX spectrometer operating at the proton frequency of 600.127 MHz, using a 5-mm selective probe equipped with a self-shielded xyz-gradient coil at 20.0 ± 0.1°C. The transmitter frequency was set on the hydrogen-deuterium water exchange signal, which was calibrated to 4.821 ppm. Correlation spectroscopy (COSY), total correlation spectroscopy (TOCSY) MLEV-17 based two-dimensional homonuclear magnetization transfer spectroscopy, using the MLEV-17 pulse scheme with 150 ms spin lock,[49] and nuclear Overhauser effect spectroscopy (NOESY) experiments with a mixing time of 150 mS, were acquired under identical conditions for all samples.[49]

Spectra were processed with TopSpin (Bruker Analytische Messtechnik GmbH) and analyzed using SPARKY software.[50] Resonance assignment followed the sequential assignment methodology developed by Wüthrich.[49, 51] Peak intensities were manually assigned as strong (from the Van der Waals radius, 1.8 Å – 2.5 Å), medium (1.8 Å – 3.5

Å), weak (1.8 Å – 4.5 Å) and very weak (1.8 Å – 5.5 Å) with a ±0.5 Å error. The three-dimensional structures of the peptides were calculated using XPLOR (version 3.856)[39] by hybrid distance geometry-dynamical simulated annealing.[49] The copper-sulfur bonds were introduced using patches within XPLOR with the stated geometry. There were 50 initial structures. The NOE energy was introduced as a square-well potential. MolMol[52] was used to create final ensembles of structures. Low energy structures chosen for further analysis had no NOE violations, deviations from ideal bond lengths of less than 0.05 Å, and bond angle deviations from ideality of less than 5º. Analyses and figures were made using Chimera.[40]

2.4. Protein Expression and Purification

Atox1 gene (gene ID 475) was purchased from IDT Ltd, codon optimized for bacterial expression and containing flanking BamH1 and Xho1 sites. The gene was sub-cloned into pETM11-Sumo3 vector (a kind gift from Dr. Huseyin Besir, Protein Expression and Purification Core Facility, EMBL), between the BamHI and XhoI sites, to construct the pETM11-Sumo3-Atox1 plasmid. Mutations were introduced by the Quikchange protocol using codon-optimized primers.[49] The chimeric His-Sumo-Atox1 protein and the mutant analogues were produced using auto-induced expression procedure as follows: pETM11-Sumo3-Atox1/mutant plasmid was freshly transformed into Escherichia coli C41 cells (Lucigen TM), and a single colony was used for initiating a 5 ml starter in LB at 37 °C for 6 h. The starter growth was subsequently used for inducing 1L of growth in auto-Induced media containing 100 µM kanamycin and formulated carbon sources according to standard procedures.[49, 53-54] Following 14 h of incubation at 37 °C at 220 rpm, cells were harvested by centrifugation and stored at -80 °C. Cell pellet from 1 L culture, was thawed on ice and re-suspend in 70 ml buffer A (25 mM HEPES pH 7.5 with 0.5 M NaCl, 10% glycerol for all proteins except for M10A: 25 mM HEPES pH 7.5 with 0.5 M NaCl, 20% glycerol, 0.5% zwittergent 3-14) supplemented with protease inhibitor cocktail 1:200, 1 mM PMSF, 50 µg/ml Dnase I, and 0.2 mg/ml lysozyme. All procedures were performed at 4 °C. Cells were lysed using a Micro-fluidizer (model M-110 EHIS; Microfluidics Corp., Newton, MA) at 21,000 psi. Insoluble cell debris was removed from the cell lysate by centrifugation at 4 °C for 15 min (15,000×g); the clear lysate was

filtered through a GF/D filter and followed by filtration using 0.45 µm filter. The filtrate supernatant was applied to a 4 ml Ni-Sepharose FF column (GE-Healthcare) in an ÄKTA Explorer system (GE-Healthcare) at 4 °C, and protein was eluted with a step gradient of imidazole in buffer A.

The fractions were analyzed on PAGE-SDS gel and OD280/260 profile, and fractions containing high concentration of eluted protein were pooled and treated with Sumo protease (2 $\mu g \cdot mL^{-1}$) for 16 h at 4 °C to cleave off the His-Sumo fusion protein. Finally, protein was precipitated with 90% ammonium sulphate (in order to concentrate the protein and eliminate electrostatic interactions between SUMO and Atox1 after cleavage) for 1 hr at 4 °C, spin 15min 13,000 rpm at 4 °C, pellet dissolved in minimal buffer, and loaded on a 200 ml Superose 30 preparative column 100×1.6 cm (GE-Healthcare) equilibrated in buffer containing 20 mM ammonium acetate pH 7.4 and 250 mM NaCl, at 4 °C. Eluted protein was pooled based on PAGE-SDS and OD280/260 profile.[49] Proteins purities were confirmed by ESI-MS[49] after dialysis for 24 h (GeBA Ltd, cutoff 1kDa) versus 20 mM ammonium acetate pH 7.4. In addition, inductively coupled plasma mass spectrometry (ICP-MS) showed the presence of only trace amounts of copper in the sample of Atox1 (<1%).

2.5. Cu(I)-DTT Complex Preparation

The Cu(I)-DTT complex was prepared as previously described,[19] from $Cu(OAc)_2$ (25 µL, 0.1 M) and DTT (75 µL, 0.1 M), diluted with 4 mL of the appropriate ammonium acetate buffer (pH 7.4 or 8.5, measured by GLP21 CRISON pH meter; final concentration of the complex is 0.61 mM).

2.6. Affinity Determination

Peptides: Each peptide was dissolved in the Cu(I)-DTT buffer solution (pH 7.4 or 8.5) to achieve a final concentration of 0.62 mM of the complex. Finally, the solution was diluted with buffer solution to a concentration of 0.16 mM. Proteins: After gel filtration, proteins concentrations were determined by UV spectrometer at 280 nm OD (10-50 µM) in 20 mM ammonium acetate buffer, pH 7.4. Half of each protein solution was adjusted

to pH 8.5 with diluted ammonium hydroxide. The solutions were diluted to a final concentration of 10 µM and 1eq of freshly prepared Cu(I)-DTT solution was added.

The solutions were injected into electrospray ion source of an API2000 instrument (Applied Biosystems) by a syringe pump at 10 $\mu L \cdot min^{-1}$. The spectra were recorded for 5 min at the m/z range of 500-1800 Da with the following instrument parameters: ion spray voltage 5500 V; curtain gas 10 $L \cdot min^{-1}$; declustering potential 40 V; focusing potential 350 V. First all solutions were tested in the absence of free DTT in order to determine the complexation percentage. Increasing concentrations of free DTT were then added separately and the solutions were incubated for 2 min at RT. Each sample was analyzed by ESI-MS (see parameters above) and the intensities of the apo and holo peaks were measured.

2.7. K_d Calculation - assuming 1:1 metal-DTT complexation (to verify reproducibility of results)[19]

Free metal concentration was calculated for each sample according to the known procedure. In addition, for each sample Y, the fractional content of the complex was calculated according to Eq. 1:

(1) $$Y = \frac{Intensity_{(holo)}}{Intesity_{(holo+apo)}}$$

Free metal concentration was plotted against Y and fitted to a hyperbolic curve using OriginPro8. The K_d value of a monomeric complexation mode equals the free metal concentration where Y = 0.5.

2.8. K_d Calculation - considering oligomeric products of metal-DTT

In order to quantify dissociation constants of Cu(I)–protein complexes, the general reaction model was used, which takes into account different protonation states of DTT and all possible complexes of Cu(I) and DTT. DTT can be found in three protonation states, characterized by two protonation reactions (reactions 2-3) and Cu(I) and DTT can form the following complexes (reactions 4-7):[55]

(2) $HDTT \rightleftharpoons DTT^- + H^+$

(3) $H2DTT \rightleftharpoons DTT^{2-} + 2H^{+}$

(4) $Cu^{+} + DTT^{2-} \rightleftharpoons CuDTT^{-}$

(5) $Cu^{+} + 2\ DTT^{2-} \rightleftharpoons CuDTT_2^{3-}$

(6) $2\ Cu^{+} + 3\ DTT^{2-} \rightleftharpoons Cu_2DTT_3^{4-}$

(7) $3\ Cu^{+} + 4\ DTT^{2-} \rightleftharpoons Cu_3DTT_4^{5-}$

The strict 1:1 Cu(I)/P (P is protein or peptide) stoichiometry was assumed for all ligands studied, as supported by ESI-MS (reaction 8):

(8) $Cu + P \rightleftharpoons Cu\text{-}P$

The dissociation constant was calculated applying the Levenberg – Marquardt algorithm[56-57] to nonlinear curve fitting, implemented in the Mathematica 9 environment. During this iterative procedure at every step the concentrations of all reagents were calculated and the minimized function was $\chi 2$ error of fitting predicted concentration of Cu-protein concentration to fractional content of the complex, calculated from experimental data, where intensities were obtained from mass spectrometry experiments. The cumulative stability constants (log β values[49]),[55] which characterize reactions 1-6 were used for calculations.

2.9. Kinetic Measurements

Peptide or protein (5 µmol) was dissolved in 2 mL TDW (2.5 mM) and reacted with 1 eq. of Cu(I)-DTT complex under inert N_2 environment, using a glove box (M Brown). The sample was analyzed by ESI-MS (API2000 Applied Biosystems) to confirm full complexation in 1:1 Cu(I)/(peptide/protein) complexation mode. UV-Vis spectrum (Genesys 10S, Thermo Scientific; VISIONlite program) was then recorded (220 – 700 nm), and 120 µL of H_2O_2 30% was added (0.5 M). Spectra were collected every two minutes for 3-15 hours, and the absorbance at λ = 298 nm, or 320 nm to vs. time was analyzed using Origin Pro8. Control measurements were conducted similarly with no metal, revealing no absorbance change.

2.10. pK_a Determination of Cys6

pK_a values were determined by spectrophotometric monitoring of SH deprotonation, using a known procedure.[49, 58-59] Stock solutions of Ala mutants C3A of the peptides MTC and MHC were prepared at concentrations of 300 mM with sodium phosphate buffer pH 6.0. Sodium borohydride was then added in excess in order to reduce the thiol group of Cys6. After dialysis into the same buffer the samples were diluted to a final concentration of 150 mM. 2 mL from these samples were monitored separately by UV spectroscopy (25 °C, Genesys 10S, Thermo Scientific; VISIONlite program) at the range of 230 – 300 nm during titration with 1 M NaOH. Simultaneously, the pH was determined by applying the exact same conditions on a second identical sample for each peptide. The absorbance at 240 nm vs. pH was analyzed using Origin Pro8 and the pK_a values were calculated from the fitted curve. All measurements were performed twice, on different days, with separate experimental setups.[49]

3. Results

3.1. Structure determination of the MHC model peptide

A head-to-tail cyclic model peptide with the sequence MHCSGCSRPG (hereby referred to as MHC) was analyzed as an exact analogue of the previously studied system, but with His rather than Thr at position II (binding sequence of Atx1, hereby referred to as MTC).[31, 33-34] The peptide was first examined in 10% D_2O in TDW at pH ~3.0, 298 K with and without the addition of one equivalent of CuCl under an inert environment. The structures were determined by NMR as previously described.[31-32, 60]

Comparing the TOCSY spectra of the apo and holo samples[49] revealed that upon addition of Cu(I), a single new species formed, evident by the significantly extended range of amide chemical shifts in the presence of Cu(I). The amide protons in the up-field region were Cys3 at 7.1 ppm and Cys6 at 7.5 ppm, which had shifted by 0.7 and 0.8 ppm upon binding, respectively. Spectral analysis using Sparky[50] and structure determination by standard methodology[51] using Xplor,[39] were initially performed on COSY, TOCSY and NOESY experiments, taken under identical conditions. Importantly, analysis and structure determination initially did not involve any metal-binding constraints to

determine which atoms were positioned at distances appropriate for metal coordination in an unbiased manner, without forcing a particular coordination mode.[60]

A total of 34 of 50 structures obtained had no violations and the low-energy ensemble chosen for analysis included ten low-energy structures with backbone and heavy atom RMSD values of 0.01 and 0.58 Å, respectively (Figure 2).

The structures showed an average distance of 3.17 ± 0.02 Å between the sulfur atoms of Cys3 and Cys6. In contrast, unlike previously observed for the analogous model MTC,[31] the average distances between the sulfur atom of Met1 and the sulfur atoms of the cysteine residues were both above 6 Å, as were the distances between both N atoms of His2 and all S atoms (Table 1). These distances are significantly longer than those indicative of binding, suggesting that, unlike the case of the MTC peptide,[31] Met1 did not bind the copper ion, and neither did the His2; only the sulfur atoms of Cys3 and Cys6 were in positions suitable for metal coordination, as reported for the natural systems.[13-15, 17-18, 20-21] Arg8 was positioned near the metal center with the average distances between its Nη and the sulfur atoms of Cys3 and Cys6 being 5.0 ± 0.2 and 3.6 ± 0.1 Å, respectively (Table 1). This distance enables it to participate as a counter ion, neutralizing the anionic charge on the ligated metal center, as reported for Lys65 in the native Atx1.[20] ESI-MS results supported mononuclear complexation.

After establishing that Cys3 and Cys6 are the coordinating residues, the calculation was repeated including bonds to Cu(I). The Cu(I)–Cys bonds were set to 2.20 ± 0.05 Å and the Cys–Cu(I)–Cys angle was 170˚ ± 5˚.[20]

A low energy ensemble of ten structures was found among the 25 non-violated of 50 total conformers (Figure 3), with backbone and heavy atom RMSD values of 0.12 and 0.50 Å, respectively. The average distances between the Cu(I) and the sulphur atom of Met1 and the nitrogen atoms of His2 were again too long to support binding (Table 1). The average distance between Nη of Arg8 and the Cu(I) was 4.7 ± 0.3 Å, supporting, again, the participation of arginine as a counter ion, especially as the corresponding distance between the Cu(I) and Lys60 in the ensemble analyzed for the natural protein Atox1 was 4.6 ± 0.3 Å (PDB accession code 1TL4)[21] (for Atox1 analogous distance to Lys65: 3.8 ± 0.5 Å; PDB accession code 1DD8).[20] Additional stabilizing interactions occurred between the side-chain oxygen of Cys3 and the amide protons of Cys6 and Gly5 in 40%

of the conformers (2.360 ± 0.001 and 1.654 ± 0.001 Å, respectively). It was noticeable that the bulky His ligand was positioned somewhere between the metal center and the non-binding Met ligand.

The NMR spectra of the peptide with Cu(I) acquired in an environment of around neutral pH (~6.7 and ~7.4) indicated formation of an identical new complex as that obtained under acidic conditions, although the spectra of the apo species were different. Increasing the pH to ~8.3 led to lack of spectral information due to rapid exchange of backbone protons with deuterium, precluding structure determination. Thus, no pH dependence was clearly identified for the coordination of this Cys-Cu(I)-Cys peptide, and as basic conditions enhances deprotonation of the Cys residues, it is unlikely that a coordination change would take place at higher pH.

The structure obtained thus presents the first Cys-Cu(I)-Cys model peptide obtained under neutral conditions, with coordination similar to that reported for related natural systems.[13-15, 17-18, 20-21] Unlike for CopZ,[48] the N atoms of the His residues did not participate in binding; nevertheless, position II impacted the binding mode to give a Cys-Cu(I)-Cys rather than Cys-Cu(I)-Met as observed under neutral conditions for the analogous MTC peptide, even without participating itself in binding; its influence may be attributed to steric effects.

3.2. Affinity and oxidative kinetic studies with Thr vs. His peptides

Affinity to Cu(I) was measured to the head-to-tail cyclic peptides MTC and MHC, in comparison to that of Atox1.[29] The Cu(I) complexes of the peptides were obtained by reacting the purified peptide with 1 eq. of freshly prepared Cu(I)-dithiothreitol (DTT) complex, and confirmed by ESI-MS to include a 1:1 Cu(I)/(peptide/protein) monomeric species.[19] Atox1 was cloned in pET-based N-terminal Sumo vector, expressed in Escherichia coli C41 strain, and Nickel purified according to manufacturer's procedures, as established based on PAGE-SDS gel, OD280/260 profile and ESI-MS spectra.[49, 53-54] The protein was reacted with 1 eq. of Cu-DTT complex to assure full Cu(I) complexation. The affinity of the peptides and protein to Cu(I) was measured according to a known well-established procedure based on mass spectrometry, analyzing binding competition between the peptides and DTT (Table 2; Figure 4[49]). [19, 61-63]

The experiments were performed at pH 7.4 and 8.5, using 20 mM ammonium acetate buffer adjusted to the desired pH with diluted ammonium hydroxide. Herein, after verifying reproducibility of results for Atox1 applying the method exactly as previously described,[19] a modified numerical model was employed to account for the major species at pH 7.4 and 8.5: Cu_2DTT_3 and $CuDTT_2$, respectively.[55, 60] The results are summarized in Table 2 (Figure 4).

When comparing the affinity of the model peptides to that of the native protein, rather similar affinities were observed for the models under basic conditions and mildly decreased ones under neutral conditions; comparing species with the same residue at position II of the binding sequence at neutral conditions, namely, Atox1 and MTC, a 6.3 fold drop in affinity resulted from eliminating the protein folding. When comparing the dissociation constants of the MTC and MHC peptides, the affinity of the MHC to Cu(I) was higher than that of MTC (Figure 4) under neutral conditions, a variation which did not exist under basic conditions. The difference between the affinity of MTC and MHC under neutral conditions is in good agreement with the determined structures: whereas MTC exhibited Met-Cu-Cys binding under these conditions (Figure 1), MHC exhibited Cys-Cu-Cys binding (Figure 3); the added covalent nature to the metal bonds may explain the stronger binding in MHC.

A further support to the effect of position II and the different S-binding residues on the peptide reactivity was obtained from comparative kinetic studies of the oxidation of the peptide-Cu(I) complexes. The peptide complexes were separately reacted with at least 200 eq. of hydrogen peroxide under pseudo-first-order Haber Weiss conditions (Eq. 1) and the UV-Vis spectra were recorded every 2 minutes for 3-15 hours. The absorbance at λ = 298 nm for peptides or λ = 320 nm for Atox1 was plotted vs. time to give $t_{1/2}$ values for metal oxidation as summarized in Table 2.[49] Notably, no change in absorbance was obtained for any of the apo-species upon addition of H_2O_2, ruling out thiolato oxidation as the source of absorbance change, thus supporting the metal center as the redox-active site. According to the kinetic results, as expected, steric bulk introduced by the protein folding contributed to the inhibition of metal oxidation. Comparing the $t_{1/2}$ values of the two peptides reveals again the impact of position II. The anionic charge of the metal center of the MHC peptide may serve as an explanation to metal oxidation occurring

more readily. Although possible participation in charge neutralization by Arg8 (Figure 3) was deduced for the MHC peptide, the analogous effect of Lys60 in Atox1 is surely more pronounced.[21] These results overall support the structural determination of the MHC and MTC peptides, the former includes two Cu(I)-Cys bonds, while the latter only a single Cu(I)-Cys bond and the less expected Cu(I)-Met bond.

3.3. pK_a determination of Cys6 side chain of Thr vs. His peptides

In order to shed more light on the role of His vs. Thr on peptide reactivity, and on the possible reasons for the reduced involvement of Cys6 in metal binding, the pK_a values of the thiol group of Cys6 were determined for Thr and His peptides. To avoid complications from the presence of another thiol group, Ala-scan mutants of C3A were employed. Whereas the His peptide exhibited a reduced pK_a compared with that of free cysteine (8.30 ± 0.01 vs. 8.37 respectively), the Thr peptide featured a markedly higher pK_a value (8.93 ± 0.08).[49] These findings may imply that His activates Cys6 and consequently lowers its pK_a, for instance, by forming H-bonding.[64] Altogether these results are consistent with binding of Cys6 under neutral conditions only for the His peptide, whereas the for the Thr peptide, Cys binding may occur only under basic conditions.

3.4. Whole-protein studies

To gain more information on participation of different residues in the binding sequence on protein structure and reactivity, three Ala-scan mutants of Atox1 with substitutions of S residues suspected in metal binding M10A, C12A, C15A, were expressed and purified similarly to Atox1 as described above. The Cu(I) complexes were prepared similarly and the affinity and the kinetic features of the mutants were also measured as described above and compared to those of Atox1 (Table 3).

As expected, the highest metal affinity was measured for the native protein Atox1. Moreover, mutating particular residues in the binding sequence of the whole proteins impacted the affinity much more drastically than did eliminating the protein fold (Tables 2, 3); up to three orders of magnitude differences were recorded. This implies participation on the mutated residues in metal binding.

Inspecting the particular K_d values calculated, it is evident that the dissociation constants for all proteins measured are between two to four orders of magnitude lower under basic conditions, supporting a possible role of pH in controlling metal affinity. Notably, replacing M10 at the conserved binding sequence with Ala decreased the affinity to Cu(I) at pH 7.4 significantly, by ca. 100-fold (Table 3).[30] Moreover, under basic conditions, the affinity of M10A was similar to that of the wild-type protein (Table 3), questioning folding alteration as a sole source for affinity drop under neutral conditions, while suggesting a possible pH-dependent change in coordination. Interestingly, precluding C12 from binding Cu(I) in the C12A mutant drastically reduced the affinity under both neutral and basic conditions by two to three orders of magnitude, whereas replacing the second Cys (C15) with Ala impacted the affinity only mildly (Table 3).[49] This emphasizes the non- equivalency of the two Cys residues.[65] a plausible explanation may relate to different participation in metal binding;[31] if C12 binds the metal under both pH conditions as observed for model peptides,[31] it is reasonable that its replacement with A will markedly impair the metal affinity under both conditions; similarly, if C15 indeed binds only under basic conditions, it is logical that its substitution induces a milder effect under neutral conditions. Notably, the different impact of the two Cys residues on affinity cannot be attributed to differences in pK_a values, as an opposite trend would be expected if any, based on the values previously reported with lower pK_a for C15.[37] Unfortunately, the affinity of the C15A mutant under basic conditions could not be determined due to low complexation in the presence of DTT. These findings overall agree with greater contribution of Met10 to the protein function than that of Cys15.

Further support to the effect of the different residues was obtained from kinetic oxidation studies (Table 3). The protein complexes were separately reacted with hydrogen peroxide as described above, and the UV-Vis spectra were recorded every 2 minutes for several hours. Stronger impact on $t_{1/2}$ values was recorded for M10 and C12, relative to C15. Again, no change in absorbance was obtained for any of the apo-proteins upon addition of H_2O_2, ruling out thiolato oxidation as the source of absorbance change. It is thus again evident that under neutral conditions, the contributions of Met and Cys12 to the complex reactivity are greater than that of Cys15.

4. Discussion

This paper describes the impact of position II in the binding sequence of metallochaperones, whether Thr or His, on metal binding and reactivity. The analyses were based on small peptide models, as well as whole proteins, at different pH conditions. When inspecting the behaviors of the MTC and MHC model peptides under different pH conditions, a correlation was observed between their binding modes as analyzed by NMR[31] and their affinities. Under neutral conditions the MHC peptide bound Cu(I) more tightly than its analogue, whereas under basic conditions the affinities of both were similar. In agreement, the NMR structures at neutral pH showed that the MHC bound the ion via two covalent bonds to Cys groups, while MTC bound it via only one covalent Cys and one coordinative Met, expected to be weaker.[31] At higher pH promoting Cys deprotonation, however, similar Cys-Cu(I)-Cys binding mode is consistent with similarly high affinity. Thus, a pH-dependent binding mode was detected for one of the models.[31-34]

As previous peptides with different residues at position II showed different coordinations,[31-32] this position is obviously crucial in determining the metal binding mode, and accordingly, the reactivity. Actually, His at position II changed the binding mode in MHC relative to MTC without participating itself in metal binding. The possible effect of position II on protein reactivity is particularly intriguing considering the differences in the Menkes and Wilson's metal binding domains: M*T*CXXC versus M*H*CXXC. It is plausible that the His residue sterically prevents the binding of Met observed in the MTC peptide, as is also supported by a recent study that described the dislocation of Met by His at the third metal binding domain of Menkes ATPase.[27] It is noteworthy though, that the sequences analyzed herein include the Atox1 binding sequence and not that of Menkes/Wilson proteins, where different X residues may also induce various effects. An alternative explanation is offered by the titration results, where H-bonding between His and Cys may lower the pK_a,[64] thus promoting deprotonation and metal binding.

The affinity studies on whole proteins pointed to markedly enhanced effect of particular residues in the binding sequence than that of the protein fold. This implies that binding affinity is mostly dominated by the metal binding site and its immediate surroundings for

this family of proteins. Nevertheless, the mild yet evident drop of affinity for the MTC peptide points to some role of the entire protein sequence in accommodating metal binding, which is surely achieved through both steric and electronic influences. Interestingly, the affinity studies conducted with the Ala protein mutants raise the possibility of Met binding also for the native system with Thr2, as observed with the peptide models. Although Met contribution to other factors essential for protein stability and reactivity is certainly reasonable, the clear effect of Met and only one of the Cys on affinity, different than that of the second Cys, only at lower pH, and stronger than that observed for eliminating protein fold, imply that Met may have bound the Cu(I) in the Atox1 protein under the experimental conditions. These findings are thus in good agreement with the results obtained with the peptide analogue, pointing to Met ability to participate in binding under particular settings.[31-32] Therefore, although some structures of the natural protein obtained upon particular Cys-Cu constraints presented Met at positions non-suitable for metal binding,[9, 11, 20, 22, 27-29] its potential coordination should not be ignored in future structural analyses that include metal-ligand binding constraints, especially as no relevant X-ray structure of a monomeric protein-Cu(I) complex has been published.

The dissociation constants measured for Atox1 and its three mutants suggest a dynamic binding mode to Cu(I) ions, where pH impacts metal affinity also in whole proteins. It is reasonable that under a proton-rich environment, Cys protonation should increase its dissociation constant, as supported by the peptide results. This is generally consistent with the hypothesis previously raised on possible pH-dependent transport mechanism.[31-32, 37] As the natural environment is different than that studied under laboratory setting, it is not unlikely that coordination variations might occur at different pH ranges, potentially promoting Met binding at particular more acidic intracellular locations. We thus may hypothesize that fine pH variations that alter the coordination modes along with the binding constants among different proteins/domains may dictate the delivery chain and release of the metal at its target location.

To conclude, the peptide with His at position II is the first fully characterized structural model for copper metallochaperone binding sites presenting the Cys-Cu(I)-Cys coordination mode, obtained under biologically relevant conditions. Importantly, based

on various similarities among model peptides and whole proteins, position II is proposed to play an important role in the copper transport in the metallochaperones, which also explains its relatively conserved nature. Additional studies are required to fully elucidate the sources of its influences and their direct impact on cellular reactivity.

5. Table of Abbreviations

Ala	Alanine
Arg	Arginine
Asp	Aspartate
Atox1	Human antioxidant protein 1
ATP7A	P-Type ATPase, Menkes' protein
ATP7B	P-Type ATPase, Wilson's disease protein
Atx1	Yeast antioxidant protein 1
CopZ	Copper transport protein
COSY	Correlation spectroscopy
Cys	Cysteine
DTT	Dithiothreitol
ESI-MS	Electrospray ionization mass spectroscopy
His	Histidine
Lys	Lysine
MBD	Metal binding domain
Met	Methionine
MHC	MHCSGCSRPG peptide
MTC	MTCSGCSRPG peptide
NOESY	Nuclear Overhauser effect spectroscopy
ROS	Reactive oxygen species
Thr	Threonine
TOCSY	Total correlation spectroscopy
ZntA	Zinc transport ATPase protein

6. References

[1] E. Madsen, J. D. Gitlin, Annual Review of Neuroscience 30 (2007) 317-337.

[2] M. Cuillel, Journal of Inclusion Phenomena and Macrocyclic Chemistry 65 (2009) 165-170.

[3] H. Tapiero, D. M. Townsend, K. D. Tew, Biomedicine & Pharmacotherapy 57 (2003) 386-398.

[4] K. A. Koch, M. M. O. Pena, D. J. Thiele, Chemistry & Biology 4 (1997) 549-560.

[5] E. D. Harris, Annual Review of Nutrition 20 (2000) 291-310.

[6] S. J. Lippard, Science 284 (1999) 748-749.

[7] M. M. O. Pena, J. Lee, D. J. Thiele, Journal of Nutrition 129 (1999) 1251-1260.

[8] K. A. Markossian, B. I. Kurganov, Biochemistry-Moscow 68 (2003) 827-837.

[9] F. Arnesano, L. Banci, I. Bertini, S. Ciofi-Baffoni, European Journal of Inorganic Chemistry (2004) 1583-1593.

[10] J. T. Rubino, K. J. Franz, Journal of Inorganic Biochemistry 7 (2012) 129-143.

[11] D. L. Huffman, T. V. O'Halloran, Annual Review of Biochemistry 70 (2001) 677-701.

[12] L. Banci, I. Bertini, K. S. McGreevy, A. Rosato, Natural Product Reports 27 (2010) 695-710.

[13] M. S. Shoshan, E. Y. Tshuva, Chemical Society Reviews 40 (2011) 5282-5292.

[14] L. A. Finney, T. V. O'Halloran, Science 300 (2003) 931-936.

[15] A. C. Rosenzweig, Accounts of Chemical Research 34 (2001) 119-128.

[16] A. K. Wernimont, D. L. Huffman, A. L. Lamb, T. V. O'Halloran, A. C. Rosenzweig, Nature Structural Biology 7 (2000) 766-771.

[17] E. Luk, L. T. Jensen, V. C. Culotta, Journal of Biological Inorganic Chemistry 8 (2003) 803-809.

[18] A. K. Boal, A. C. Rosenzweig, Chemical Reviews 109 (2009) 4760-4779.

[19] L. Banci, I. Bertini, S. Ciofi-Baffoni, T. Kozyreva, K. Zovo, P. Palumaa, Nature 465 (2010) 645-648.

[20] F. Arnesano, L. Banci, I. Bertini, D. L. Huffman, T. V. O'Halloran, Biochemistry 40 (2001) 1528-1539.

[21] I. Anastassopoulou, L. Banci, I. Bertini, F. Cantini, E. Katsari, A. Rosato, Biochemistry 43 (2004) 13046-13053.

[22] L. Banci, I. Bertini, S. Ciofi-Baffoni, D. L. Huffman, T. V. O'Halloran, Journal of Biological Chemistry 276 (2001) 8415-8426.

[23] L. Banci, I. Bertini, R. Del Conte, M. D'Onofrio, A. Rosato, Biochemistry 43 (2004) 3396-3403.

[24] T. M. DeSilva, G. Veglia, S. J. Opella, Proteins-Structure Function and Bioinformatics 61 (2005) 1038-1049.

[25] L. Banci, I. Bertini, F. Cantini, M. Migliardi, A. Rosato, S. L. Wang, Journal of Molecular Biology 352 (2005) 409-417.

[26] L. Banci, I. Bertini, F. Cantini, N. DellaMalva, T. Herrmann, A. Rosato, K. Wurthrich, Journal of Biological Chemistry 281 (2006) 29141-29147.

[27] D. Poger, J. F. Fuchs, H. Nedev, M. Ferrand, S. Crouzy, Febs Letters 579 (2005) 5287-5292.

[28] A. Rodriguez-Granillo, P. Wittung-Stafshede, Journal of Physical Chemistry B 13 (2009) 1919-1932.

[29] A. C. Rosenzweig, D. L. Huffman, M. Y. Hou, A. K. Wernimont, R. A. Pufahl, T. V. O'Halloran, Structure 7 (1999) 605-617.

[30] F. Hussain,J. S. Olson, P. Wittung-Stafshede, Proceedings of the National Academy of Sciences of the United States of America 105 (2008) 11158-11163.

[31] M. S. Shoshan, D. E. Shalev, W. Adriaens, M. Merkx, T. M. Hackeng, E. Y. Tshuva, Chemical Communications 47 (2011) 6407-6409.

[32] M. S. Shoshan, D. E. Shalev, E. Y. Tshuva, Inorganic Chemistry 52 (2013) 2993-3000.

[33] O. Seneque, S. Crouzy, D. Boturyn, P. Dumy, M. Ferrand, P. Delangle, Chemical Communications (2004) 770-771.

[34] P. Rousselot-Pailley, O. Seneque, C. Lebrun, S. Crouzy, D. Boturyn, P. Dumy, M. Ferrand, P. Delangle, Inorganic Chemistry 45 (2006) 5510-5520.

[35] S. Zeevi, E. Y. Tshuva, European Journal of Inorganic Chemistry (2007) 5369-5376.

[36] A. Kohner-Kerten, E. Y. Tshuva, Journal of Organometallic Chemistry 693 (2008) 2065-2068.

[37] A. Badarau, C. Dennison, Journal of the American Chemical Society 133 (2011) 2983-2988.

[38] L. Banci, I. Bertini, S. Ciofi-Baffoni, L. A. Finney, C. E. Outten, T. V. O'Halloran, Journal of Molecular Biology 323 (2002) 883-897.

[39] M. Nilges, J. Kuszewski, A. T. Brunger, Sampling properties of simulated annealing and distance geometry. Plenum Press: New York (1991).

[40] E. F. Pettersen, T. D. Goddard, C. C. Huang, G. S. Couch, D. M. Greenblatt, E. C. Meng, T. E. Ferrin, Journal of Computational Chemistry 25 (2004) 1605-1612.

[41] K. Arumugam, S. Crouzy, Biochemistry 51 (2012) 8885-8906.

[42] J. R. Forbes, G. Hsi, D. W. Cox, Journal of Biological Chemistry 274 (1999) 12408-12413.

[43] F. Arnesano, L. Banci, I. Bertini, S. Ciofi-Baffoni, E. Molteni, D. L. Huffman, T. V. O'Halloran, Genome Research 12 (2002) 255-271.

[44] J. R. Forbes, D. W. Cox, Human Molecular Genetics 9 (2000) 1927-1935.

[45] B. Sarkar, Journal of Inorganic Biochemistry 79 (2000) 187-191.

[46] P. Delangle, E. Mintz, Dalton Transactions 41 (2012) 6359-6370.

[47] C. Singleton, N. E. Le Brun, Biometals 20 (2007) 275-289.

[48] S. Hearnshaw, C. West, C. Singleton, L. Zhou, M. A. Kihlken, R. W. Strange, N. E. Le Brun, A. M. Hemmings, Biochemistry 48 (2009) 9324-9326.

[49] See Supporting Information for details.

[50] T. D. Goddard, D. G. Kneller, SPARKY 3. University of California ,San Francisco.

[51] K. Wüthrich, NMR of Proteins and Nucleic Acids (1986).

[52] R. Koradi, M. Billeter, K. Wuthrich, Journal of Molecular Graphics 14 (1996) 51.

[53] http//:wolfson.huji.ac.il/expression/procedures/bacterial/AutoInduced-Media.pdf.

[54] F. W. Studier, Protein Expresion and Purification 41 (2005) 207-234.

[55] A. Krezel, W. Lesniak, M. Jezowska-Bojczuk, P. Mlynarz, J. Brasun, H. Kozlowski, W. Bal, Journal of Inorganic Biochemistry 84 (2001) 77-88.

[56] K. Levenberg, The Quarterly of Applied Mathematics 2 (1944) 164-168.

[57] D. W. Marquardt, Journal of the Society for Industrial and Applied Mathematics 11 (1963) 431-441.

[58] J. W. Donovan, Biochemistry 3 (1964) 67-74.

[59] J. C. Lim, J. M. Gruschus, G. Kim, B. S. Berlett, N. Tjandra, R. L. Levine, Journal of Biological Chemistry 287 (2012) 25596-25601.

[60] M. S. Shoshan, D. E. Shalev, E. Y. Tshuva, Journal of Visualized Experiments (2013) e50747.

[61] L. Banci, I. Bertini, S. Ciofi-Baffoni, T. Hadjiloi, M. Martinelli, P. Palumaa, Proceedings of the National Academy of Sciences of the United States of America 105 (2008) 6803-6808.

[62] L. Banci, I. Bertini, S. Ciofi-Baffoni, I. Leontari, M. Martinelli, P. Palumaa, Proceedings of the National Academy of Sciences of the United States of America 104 (2007) 15-20.

[63] P. Palumaa, L. Kangur, A. Voronova, R. Sillard, Biochemistry Journal 382 (2004) 307-314.

[64] T. K. Harris, G. J. Turner, Lubmb. Life 53 (2002) 85-98.

[65] M. S. Koay, B. M. G. Janssen, M. Merkx, Dalton Transactions 42 (2013) 3230-3232.

Table 1. Average distances between the nitrogen and sulfur atoms of Cys, Met, His, and Arg residues of the peptide complex as calculated without metal binding constraints and between these atoms and the Cu(I) as calculated with metal binding constraints [*,†]

Peptide complex without binding constraints	
Heteroatoms[‡]	distance (Å) (STD)[#]
$S_{M1}\cdots S_{C3}$	7.53 (0.01)
$S_{M1}\cdots S_{C6}$	6.10 (0.00)
$S_{C3}\cdots S_{C6}$	*3.17 (0.02)*

$N_{H2}\cdots S_{C3}$	6.5 (0.6)
$S_{C6}\cdots N\eta_{R8}$	3.6 (0.1)
Peptide complex with metal binding constraints	
metal-heteroatom‡	distance (Å) (STD)
$Cu\cdots S_{M1}$	6.71 (0.05)
$Cu–S_{C3}$	*≡2.22*
$Cu–S_{C6}$	*≡2.22*
$Cu\cdots N_{H2}$	5.6 (0.2)
$Cu\cdots N_{R8}$††	4.7 (0.3)

***** Distances indicative of metal binding are italicized

† Set distances are prefixed with an equivalence sign (≡) and italicized

‡ Single letter abbreviation of amino acids

Where more than a single donor atom exists, the value represents the shortest distance obtained

†† Nη

Table 2. Cu(I) dissociation constants (K_d)* and $t_{1/2}$ values of Cu(I) complex oxidation with H_2O_2 for Atox1 and the model peptides MTC and MHC†

		Atox1	MTC	MHC
K*d* (aM) (R^2)‡	pH 7.4	4.8±1.4 (0.98)	30.2±8.7 (0.98)	7.6±1.3 (0.98)
	pH 8.5	0.07±0.01 (0.88)	0.14±0.07 (0.96)	0.09±0.02 (0.97)
$t_{1/2}$ (min)#		270	100	10

***** Based on the modified method taking into consideration oligomeric species of Cu-DTT[19, 55, 60]

† Conditions: 20 mM ammonium acetate, adjusted to desired pH with diluted ammonium hydroxide, 25 °C.

‡ R^2 describes the quality of the fit to the hyperbolic equation (Mathematica).

200 eq. H_2O_2, λ = 298 or 320 nm

Table 3: Cu(I) dissociation constants (K_d)* and $t_{1/2}$ values for Atox1 and its Ala-scan mutants†

		Atox1	M10A	C12A	C15A
K*d* (aM) (R^2)‡	pH 7.4	4.8±1.4 (0.98)	370±150 (0.95)	3500±1700 (0.96)	65±27 (0.94)
	pH 8.5	0.07±0.01 (0.88)	0.09±0.06 (0.88)	5.4±3.9 (0.86)	- ††
$t_{1/2}$ (min)#		270	33	25	113

* Based on the modified method taking into consideration oligomeric species of Cu-DTT[55]

† Conditions: 20 mM ammonium acetate, adjusted to desired pH with diluted ammonium hydroxide, 25 °C.

‡ R^2 describes the quality of the fit to the hyperbolic equation (Mathematica).

200 eq. H_2O_2, λ = 320 nm

†† Low complexation (below 30%), therefore no calculations could be performed.

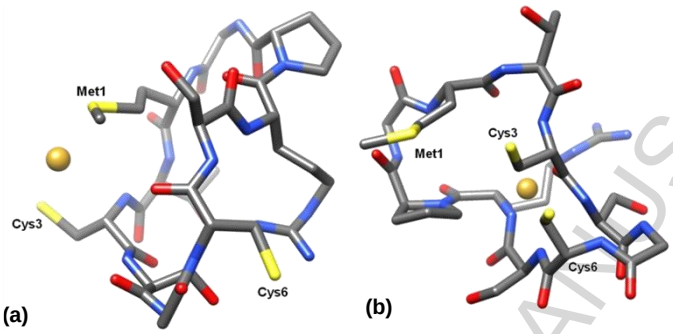

Fig. 1 Lowest energy structures of the head-to-tail cyclic peptide *MTCSGCSRPG* reacted with Cu(I) under (a) pH 3.0 and 6.7 including Met,Cys copper binding; (b) pH 8.5 including Cys,Cys copper binding (calculated using Xplor[39], analyzed and presented with Chimera[40]).[31]

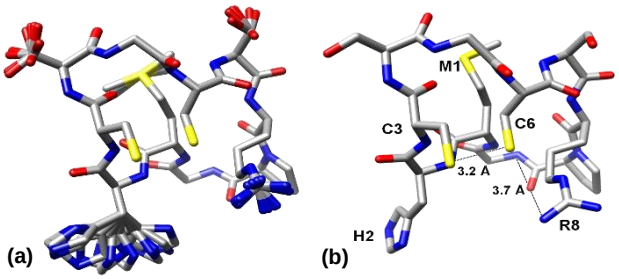

Fig. 2 (a) Superposition of ten low-energy NMR-derived structures of the MHC peptide, without Cu(I) constraints; (b) lowest energy structure showing distances between sulfur atoms of Cys residues and nitrogen Nη atom of Arg (calculated using Xplor,[39] analyzed and presented with Chimera[40]). 2.5 μmol of peptide were dissolved and reacted with stock solution of CuCl in TDW (45 μL, 56 mM) (final peptide and CuCl concentrations: 5 mM each)

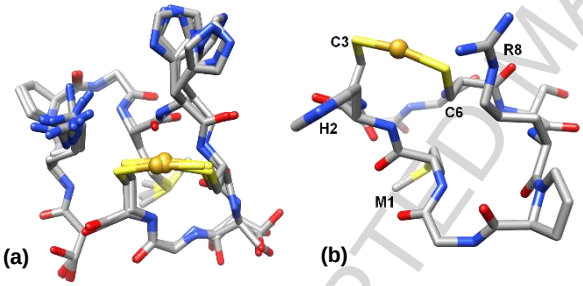

Fig. 3 (a) Superposition of ten low-energy NMR-derived structures of the MHC peptide, with Cu(I) constraints; (b) lowest energy structure (calculated using Xplor,[39] analyzed and presented with Chimera[40]). 2.5 μmol of peptide were dissolved and reacted with stock solution of CuCl in TDW (45 μL, 56 mM) (final peptide and CuCl concentrations: 5 mM each)

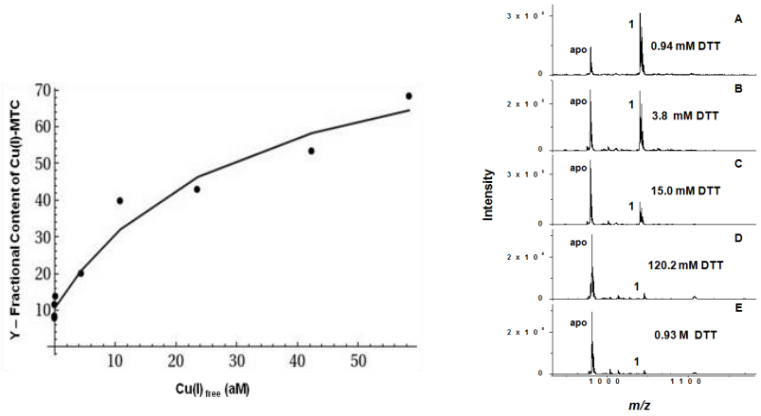

Fig. 4 K_d of Cu(I)MTC at pH 7.4, 25 °C – representative example.[49] ESI-MS spectra of Cu(I)MTC in the presence of 0.94 mM - 0.93 M DTT (*z*=5) (right); and fractional content of Cu(I)MTC dependence on concentration of free Cu(I) ions as calculated based on the consideration of oligomeric products of Cu-DTT (left).

Graphical abstract

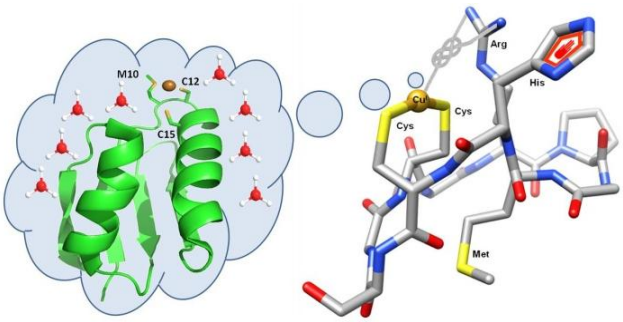

Position II in metallochaperone model peptides, whether Thr or His, affects binding mode, Cu affinity, and oxidation rate. Met binding for the Thr peptide under neutral-acidic conditions agrees with lower affinity, and together with affinity drop in a Met-mutated mettalochaperone proteins, imply that Met binding is possible under particular conditions.

Highlights

- Metallochaperone model peptide with His at position II shows Cys-Cu-Cys binding.
- Lower affinity for the Thr peptide reflects weaker binding of Cys,Met.
- Mutants of antioxidant 1 (Atox1) protein show higher impact of Met vs. Cys6 on affinity.
- pH plays a role in determining binding mode and reactivity.